J. Civil Eng. Mater.App. 2022 (December); 6(4): 229-246

Journal of Civil Engineering and Materials Application

Journal home page: http://jcema.com

Received: 04 August 2022 • Accepted: 17 November 2022

Research

doi: 10.22034/jcema.2023.384975.1103

Numerical Investigation of Steel Moment-Resisting Frame with RBS Connections under Fire Conditions

Saba Haghighat [1], Hamid Saberi [2], Vahid Saberi [2]*, Abbasali Sadeghi [3]

[1] Department of Civil Engineering, University of Eyvanekey, Semnan, Iran.
[2] Assistant Professor, Department of Civil Engineering, University of Eyvanekey, Semnan, Iran.
[3] Department of Civil Engineering, Mashhad Branch, Islamic Azad University, Mashhad, Iran.

*Correspondence should be addressed to Vahid Saberi, Department of Civil Engineering, University of Eyvanekey, Semnan, Iran. Tel: + 09366671575; sss1991b@yahoo.com.

ABSTRACT

Recent earthquakes indicate that the welding connections of steel moment-resisting frames (SMRFs) are so brittle. Then, huge damages are generated by cracking the weld between the beam flange and column face. After the 1994 Northridge and the 1995 Kobe earthquakes, reduced beam section (RBS) connections were proposed to reduce the damages by forming a plastic hinge outside the panel zone. Thus, with the great effect of seismic performance and ductility of the panel zone, RBS moves the formation of the plastic hinge at a suitable distance from the column face. In this regard, in order to evaluate the behavior of SMRF with RBS connections under fire conditions, four types of steel frame connections, including RBS with radial, rectangular, triangular, and trapezoidal cuts, were modeled in ABAQUS software. Due to the fact that fire is an unpredictable phenomenon, both in terms of size and fire load, it has special complexities. ¬The fire load was simulated either by a steady state method to reach a fully-developed fire or by a transient state method following the standard temperature–time curve. The results of this study showed that by increasing the temperature of the heated area, the transferring of the plastic hinge is conducted better. Meanwhile, based on the obtained outputs of displacement-time coefficients, the Frame-RBS-01 sample had the most ultimate strength compared to other samples up to 748.34 ° C temperature, and the least ultimate strength is related to the Frame-RBS-Rectangle-02 sample up to 526/90 ° C temperature.

Keywords: **Steel moment-resisting frame (SMRF), RBS connection, Fire, ABAQUS software.**

1. INTRODUCTION

Recent Steel connections are critical in steel frames that are subjected to loading at both ambient and high temperatures. Indeed, the susceptibility of a steel structure to failure or collapse, particularly when exposed to fire, is mainly dependent on the robustness of the connections; hence, structural behavior of connections is a major study subject that has continued to draw substantial interest. Fire intentionally or inadvertently affects the behavior of structures. Due to the significant reduction of steel strength at high temperatures, the sensitivity of steel structures to such events like fire is much higher than other structures. The current building codes and regulations define the fire resistance of steel structures by specifying parameters [1]. In various regulations and researches, some fire curves are considered to be applied to structures, while they should be noted that several parameters are effective for finding these curves. Although many regulations have been

prepared to deal with possible structural accidents, it is vital to be noted that the existing regulations have been prepared either to design structures versus earthquakes or to study the resistance of members against fire loading [2,3]. However, the combination of these two events is not considered to design a structure. Observations show that many structures are still stable and usable after fire exposure. If a structure is placed against fire before experiencing an earthquake, the structure will behave differently in a state in which no fire has occurred due to the residual stresses and strains caused by fire [4]. Steel buildings in the modern day must be resistant to a wide range of loads, including fire. Estimating the resistance of steel connections to fire or thermal stress has become a critical topic in recent years. In recent years, a significant lot of research has been conducted to better understand the behavior of structures in fire conditions and to give design recommendations for determining the degree of fire resistance in structures. This has been complemented by the creation of trustworthy design requirements such as Eurocode [5, 6], AISC [7]. A fire is a severe burning of fuel, or an unwanted, uncontrolled fire that is usually accompanied by excessive smoke and light. During a fire, part of the heat from the fire is released into the burning space and the rest is absorbed by building materials and members. As a result, structural members lose their mechanical strength and they are damaged at a critical temperature. The amount of damage caused by fire is directly related to the duration and temperature of fire loading. The duration that the material, or a combination thereof, is capable of withstanding direct fire resistance in accordance with a standard fire test. Fire resistance plays an important role in ensuring an adequate level of safety for any building. According to European standards [5], the fire loading was simulated either by a steady state method to reach a fully-developed fire or by a transient state method following the standard temperature–time curve. In the following, the research background is presented. Ali et al. studied the effects of fire in a one-story frame. Their purpose was to investigate the effect of fire scenarios on the lateral displacement of the frame as well as the type of damage caused by it [8]. In recent years, the behavior of steel structures against post-earthquake fire has also been highly regarded by researchers. Memari et al. investigated the behavior of steel moment-resisting frames (SMRFs) by connecting beams with a reduced cross-sectional area exposed to post-earthquake fire and finally concluded that these types of structures are resistant to post-earthquake fire [9]. Behnam et al. examined a 10-story SMRF exposed to fire after an earthquake [10]. Keller and Pessiki also investigated the damage caused by post-earthquakes fire-resistant coatings and its effect on the performance of steel frames in post-earthquake fire using numerical simulations [11]. The studies of Sun et al. are among the first studies to evaluate the progressive collapse of steel frames due to the failure of a column subjected to fire conditions. By using nonlinear static and dynamic analyses, they studied the progressive collapse of frames under fire loadings [12-16]. With the aim of improving the simulation of steel joints exposed to fire, Strejček et al. presented a report on the behavior of column web component of steel beam-to-column joints at elevated temperatures [17]. Jiang et al. investigated the progressive collapse of two-dimensional steel frames when a column is exposed to different temperatures by explicit dynamic analysis [18]. Guo and Huang assessed the behavior of steel beams with RBS connection under the influence of heat. The results of this study showed that by increasing rotational and axial ductility, the fire resistance in this type of connection is increased [19]. Jiang et al. investigated the effect of damping as well as the influence of strain rate on the occurrence of progressive collapse in steel frames under fire conditions. The results of their modeling showed that in damping ratios of zero to 10%, the effect of damping on the occurrence of progressive collapse in steel structures can be ignored [20]. Gernay and Gamba also studied the tensile residual force in a column under concentrated fire loading. They used natural fire diagrams to simulate fire loads to assess the effects of it on progressive collapse [21]. Khizab et al. analyzed the steel structures with SMRF in two states with and without steel plate shear wall under blast loading in two scenarios inside and outside the frame in finite element software [22]. Miryoysefi Aval and Shakeri have studied the general behavior of SMRFs under different fire scenarios through analytical models. The results showed that depending on the scenario of fire load and the ratio of gravity loads, SMRFs fail in different collapse modes [23]. Ghasemi has studied the effect of fire on the performance of special steel moment frames. For this purpose, different scenarios such as changing the position of fire in different spans and floors were examined. Thermal analysis and nonlinear analysis and finally the performance of the structures were performed using thermally modified steel materials. The results indicated that the fire in the outer span of the building will create a critical situation [24]. Sadeghi et al. investigated the reliability evaluation of SMRFs under heavy vehicle impact loadings by Monte Carlo Simulation (MCS). To reduce computational costs, meta-model techniques such as Kriging, Polynomial Response Surface Methodology (PRSM) and Artificial Neural Network (ANN) are applied and their efficiency is assessed. Also, single and multi-objective optimization of SMRFs under vehicle impact are performed by using evolutionary algorithms [25, 26].

The fire resistance of beam-to-column connections is an essential factor to consider when designing SMRFs. The authors want to investigate the effect of fire on RBS connections using finite element modeling. In this study, as a novelty, the performance of SMRF with RBS connection under fire conditions is discussed. For this purpose, four types of SMRF connections including RBS with radial, rectangular, triangular and trapezoidal cuts

were considered in ABAQUS software [27]. As a result, the most suitable type of RBS connection is determined under fire loading.

2. MATERIALS AND METHODS

SMRF system is a set of beams and columns linked to each other by rigid connections. In this system, no braces and shear walls are used, and the lateral loads are borne by the bending behavior of the connections. SMRFs create free architectural spaces with minimal structural interference. This system is used in office buildings that usually need flexible spaces with various uses. The designs are based on the details of the welded beam connections to the standard column. The supports of the columns are fixed. Buildings are controlled for a relative displacement limit of h/400, where h is the story height [28]. The design philosophy of moment frames is to eliminate the energy generated by earthquakes in plastic areas, which are generally formed inside the beams and the connection zone. Beam joints to columns are usually designed to remain elastic. Therefore, the structural shapes in the SMRF should correspond to the thickness-related constraints of the cross-sectional compaction so that the plastic joint is created without any possibility of sudden failure in the cross-section. In addition to these requirements, the frame must be composed in such a way that no soft and weak stories are created. New performance-based design guidelines, such as FEMA356 [29], have special attention to nonlinear analysis methods. Today, steps have been taken in the new seismic regulations, and design based on performance level has become the basis of these regulations [30]. In the design of members and connections of this type of frame, stricter requirements are considered compared to ordinary SMRFs. As stated in the definition of SMRF with intermediate ductility, the connections of these frames must be able to withstand at least 0.02 radians without a significant reduction in strength. In designing the connection of the beam to the column for bending and shear, either the requirements of special SMRFs can be observed or the moment and shear created in the connection under the effect of the intensified earthquake load, each of which is smaller, can be used [31].

2.1. DETAILS OF THE STUDIED SAMPLES

ABAQUS software [27] is used for various numerical modeling for nonlinear analyses. This research first presents the specifications of the used steel material and the studied models. Then the modeling method and parameters considered for the analysis of the steel models and the steps of the analysis are described. In this study, to evaluate of the performance of SMRF with RBS connection under fire conditions is discussed. For this purpose, four types of SMRF connections, including RBS with radial, rectangular, triangular, and trapezoidal cuts, were selected in ABAQUS software [27]. To design the dimensions of RBS connections, FEMA350 [32] has been used in which the allowable range for starting cut of RBS area, length, depth, and radius have been specified based on Figure 1 and Table 1. Meanwhile, the configuration of samples is indicated in Table 2.

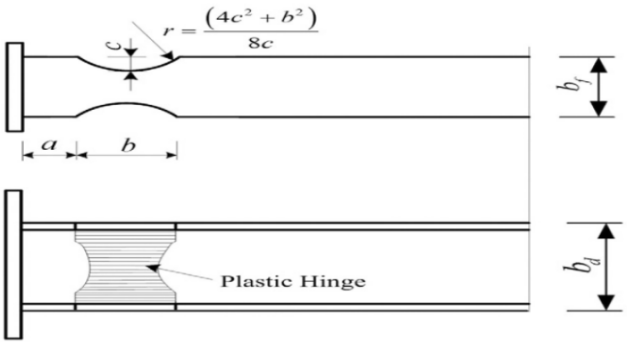

Figure 1. The parameters of RBS connection presented based on FEMA350 [32].

Table 1. The simulated samples.

Group	Sample	a	b	c	Connection Type
***RBS* with radial cut**	**Frame-*RBS*-01**	**185**	**600**	**65**	**Welded**
	Frame-*RBS*-02	**195**	**700**	**75**	**Welded**
***RBS* with rectangular cut**	**Frame-*RBS*-Rectangle-01**	**185**	**600**	**65**	**Welded**
	Frame-*RBS*-Rectangle-02	**195**	**700**	**75**	**Welded**
***RBS* with triangular cut**	**Frame-*RBS*-Triangle-01**	**185**	**600**	**65**	**Welded**
	Frame-*RBS*-Triangle-02	**195**	**700**	**75**	**Welded**
***RBS* with trapezoidal cut**	**Frame-*RBS*-Trapezoid-01**	**185**	**600**	**65**	**Welded**
	Frame-*RBS*-Trapezoid-02	**195**	**700**	**75**	**Welded**

Table 2. The configuration of samples**.**

Sample	Configuration
Frame-*RBS*-01	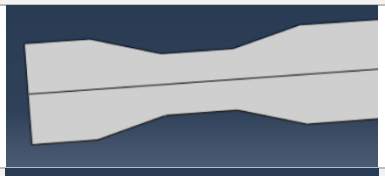
Frame-*RBS*-02	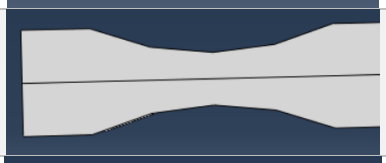
Frame-*RBS*-Rectangle-01	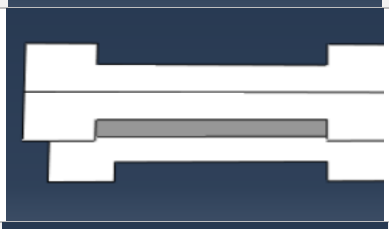
Frame-*RBS*-Rectangle-02	
Frame-*RBS*-Triangle-01	
Frame-*RBS*-Triangle-02	
Frame-*RBS*-Trapezoid-01	
Frame-*RBS*-Trapezoid-02	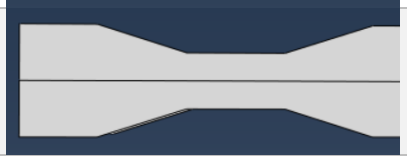

2.2. MODELING VERIFICATION

In this research, two modeling verifications, such as modeling of thermal loading and RBS connections, are presented to evaluate the performance of SMRFs with RBS connections under fire conditions based on the research of Rahnavard and Thomas [33] and Swati and Gaurang [34], respectively.

2.2.1. MODELING VERIFICATION UNDER THERMAL LOADING

This study used the results of Rahnavard and Thomas's research [33] to verify the models. After modeling the steel frame sample with the connections in the reference paper [33], the Von Mises stress contour is presented according to Figure 2. According to Figure 3, the results of the final load-vertical displacement in the middle of the span and the axial force of the screws in this study are in good agreement with the results of the reference paper [33]. The difference between the verification results is a maximum of 10%, which is considered desirable in accordance with the existing criteria for modeling accuracy.

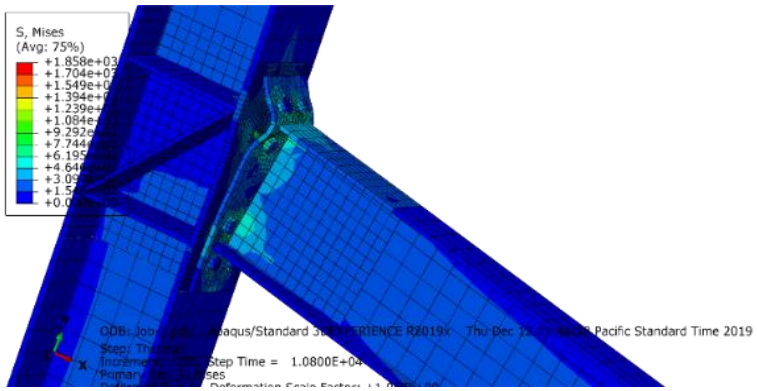

Figure 2. The Von Mises stress contour of connection under thermal loading.

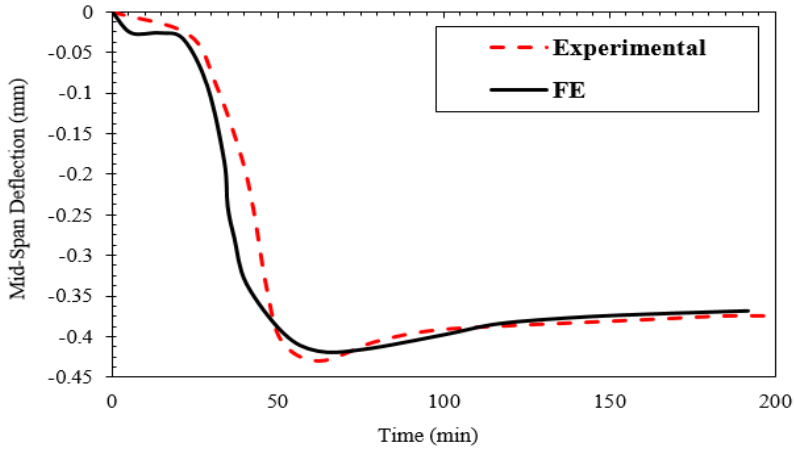

Figure 3. The accuracy of finite element modeling versus experimental result.

2.2.2. MODELING VERIFICATION OF RBS CONNECTION

In Swati and Gaurang's experimental research in 2014 [34], the RBS model was investigated under cyclic loading, and its hysteresis curve was extracted. The location and size of the RBS determined the stress level on the beam and column flanges. The overall goal in determining the RBS cut size was to limit the maximum bending of the beam that can be transmitted to the column surface by 85% to 100% of the plastic anchor on the beam. The experimental sample of RBS is also shown in Figure 4 under lateral displacement. According to Figure 5, the numerical results of the present study showed that the performance of the RBS moment connection cycles is obtained according to the experimental analysis. Also, no welding rupture was observed in the RBS connection. Based on Figure 6, the results show that the difference between the maximum values is less than 10%.

Figure 4. The experimental sample of RBS [34].

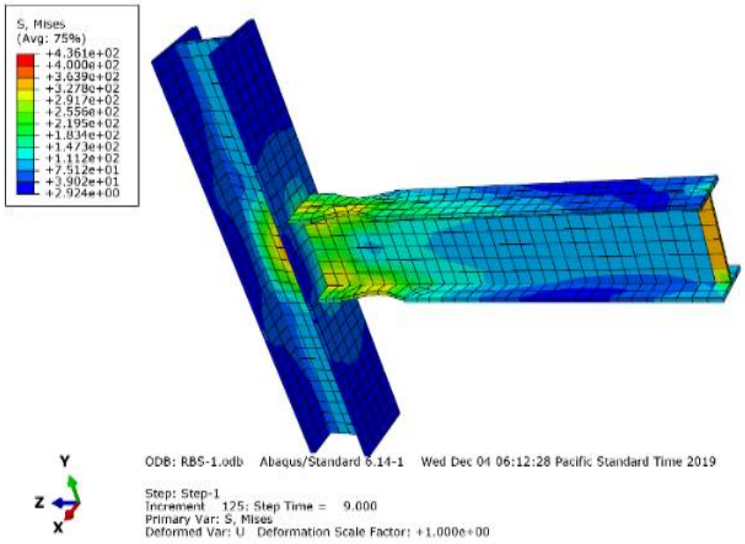

Figure 5. The Von Mises stress contour of connection under thermal loading.

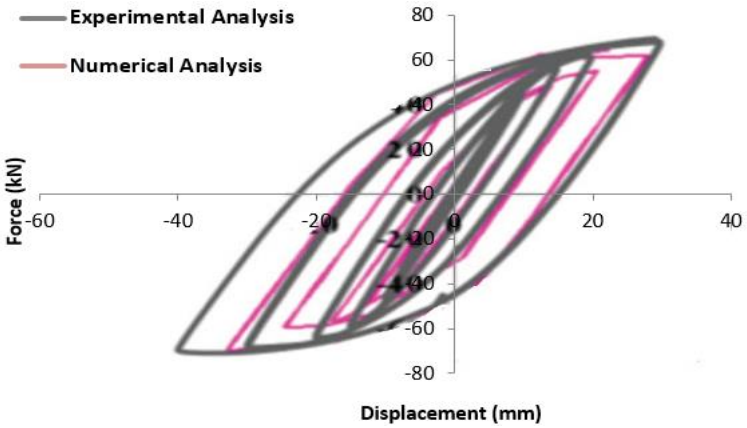

Figure 6. The accuracy of numerical modeling versus experimental result.

2.3. MODELING PROCEDURE

In order to achieve the objectives of this research, an SMRF with dimensions of 4000x3500 mm has been considered based on Figure 7. The height of the column is 3500 mm, and the length of the beam is 4000 mm. The dimensions of the column are H700x300x13, and the dimensions of the beam are H428x407x20. Dead and live loads are 500 and 200 kg/m, respectively. Due to the fact that fire is an unpredictable phenomenon, both in terms of size and load of fire, it has special complexities [35]. On the other hand, the factors affecting this phenomenon are very diverse. The most important of these factors are fire scenarios and temperature-time curves and, consequently, the fire load that is transmitted to the structure. The method used to solve thermomechanical problems. In the first stage, the structure is subjected to gravity loads, which include dead load and live load, and in the second stage, the structure is analyzed based on fire scenarios applied to it. In this step, time-temperature curves related to the chamber to apply fire are utilized. Among the yield criteria, the Von Mises criterion has been used. Of course, some other failure indices, such as plastic strain, have also been studied, which will be mentioned in the results

section. In general, the use of two types of kinematic and isotropic hardening is common for materials. In this model, hardening is considered isotropic. Thus, as the material hardens, the area of the yield circle will not change, and the yield zone will move in the direction of the axes.

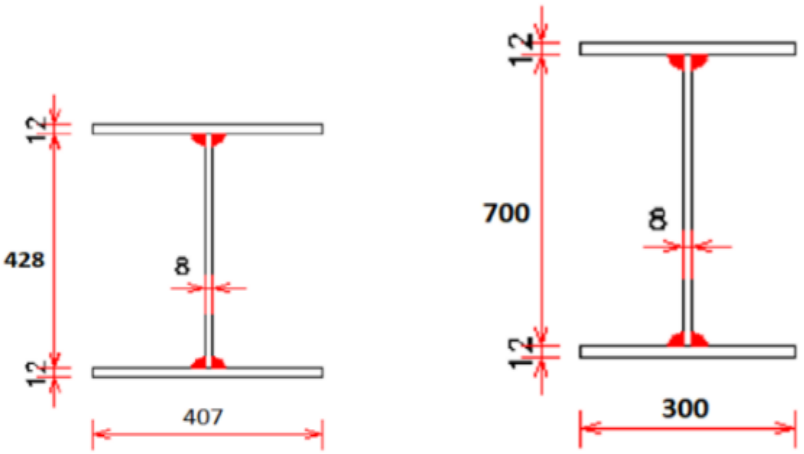

Figure 7. The used beam and column sections for *SMRF*

Among the submission criteria, the Von Mises criterion has been used. But some other indicators of failure, such as plastic strain, have also been examined, which will be mentioned in the results section. It is clear that the properties of steel exposed to fire change; these changes can be calculated according to the existing temperature, the rules and coefficients of which are given in EC3 regulations [5]. The specific heat of steel in the temperature range of 900 to 1200 ° C reaches its minimum value of 65, which is fixed in this range, and no significant decrease occurs with increasing temperature. The thermal conductivity of steel also decreases with increasing temperature until it is fixed in the temperature range of 800 to 1200 ° C and reaches its lowest value of 27.3. The values of Young's modulus and Poisson's ratio for different temperatures are presented based on Table 3. Also, the stress and strain values for different temperatures are indicated in Table 4.

Table 3. The values of Young's modulus and Poisson's ratio for different temperatures [5].

Young's modulus (N/m^2)	Poisson's ratio	Temp (C)
2.1E+11	0.3	20
2.1E+11	0.3	100
1.89E+11	0.3	200
1.68E+11	0.3	300
1.47E+11	0.3	400
1.26E+11	0.3	500
65100000000	0.3	600
27300000000	0.3	700
18900000000	0.3	800
14175000000	0.3	900
9450000000	0.3	1000
4725000000	0.3	1100

Table 4. The stress and strain values for different temperatures [5].

Stress (Pa)	Plastic strain	Temp (C)
280000000	0	20
280000000	0.001666667	20
224000000	0.158666667	20
168000000	0.168666667	20
112000000	0.178666667	20
56000000	0.188666667	20
280000000	0	100

280000000	**0.118666667**	**100**
280000000	**0.128666667**	**100**
280000000	**0.138666667**	**100**
280000000	**0.148666667**	**100**
168000000	**0.168666667**	**100**
112000000	**0.178666667**	**100**
56000000	**0.188666667**	**100**
249200000	**0**	**200**
257246996	**0.000681481**	**200**
261812804.4	**0.001681481**	**200**
264968631.4	**0.002681481**	**200**
267449732.7	**0.003681481**	**200**
269501664	**0.004681481**	**200**
271243123.2	***0.005681481***	***200***
218400000	***0***	***300***
234222853.9	***0.0007***	***300***
243353931.3	**0.0017**	**300**
249696294.6	**0.0027**	**300**
254690745.7	**0.0037**	**300**
182000000	**0**	**400**
207177074.8	**0.000761905**	**400**
148400000	**0**	**500**
167413704.4	**0.000822222**	**500**
84000000	**0**	**600**
95656652.85	**0.000709677**	**600**
36400000	**0**	**700**
42720050.31	**0.000666667**	**700**
47051011.03	**0.001666667**	**700**
50055569.38	**0.002666667**	**700**
19600000	**0**	**800**
22885036.45	**0.000962963**	**800**
24365436.04	**0.001962963**	**800**
25446477.31	**0.002962963**	**800**
30800000	**0.128962963**	**800**
14000000	**0**	**900**
14881778.91	**0.001012346**	**900**
16800000	**0.019012346**	**900**
16800000	**0.029012346**	**900**
8400000	**0**	**1000**
9311995.8	**0.001111111**	**1000**
9655506.786	**0.002111111**	**1000**
5600000	**0**	**1100**
5600000	**0.000814815**	**1100**
2240000	**0.178814815**	**1100**
1120000	**0.188814815**	**1100**

The reduction coefficients for the yield strength of the relative strength and Young's modulus in steel under high temperatures are given in accordance with EC3 [5]. By using the reduction coefficients, the unknown parameters at different temperatures that exist in the case of a fraction can be obtained from the known parameters at room temperature (20 ° C) that are at the denominator of the fraction. As can be seen in Tables 3 and 4, Young's modulus and relative limit start to decrease in the temperature range of 100 to 200 ° C, and the yield strength decreases in the temperature range of 400 to 500 ° C. At a temperature of 1200 ° C, the reduction coefficients of the

steel reach zero, which indicates that the steel no longer shows strength. Also, the thermal expansion and thermal conductivity coefficient of the steel frame are indicated based on Tables 5 and 6, respectively. Meanwhile, the specific heat of ordinary steel and stainless steel at high temperatures are depicted based on Figures 8 and 9.

Table 5. Thermal expansion coefficient for steel frame [5].

Temp (C)	expansion coefficient (1/C)
1.11E-05	20
1.11E-05	100
1.11E-05	200
1.11E-05	300
1.11E-05	400
1.11E-05	500
1.11E-05	600
1.11E-05	700
1.11E-05	800
1.11E-05	900
1.11E-05	1000
1.11E-05	1100
1.11E-05	1200

Table 6. Thermal conductivity coefficient for steel frame [5].

Temperature (C)	Thermal conductivity (W/mK)
48	0
47.56	20
45.8	100
43.6	200
41.4	300
39.2	400
37	500
34.8	600
32.6	700
30.4	800
28.2	900
28.2	1000
28.2	1100
28.2	1200

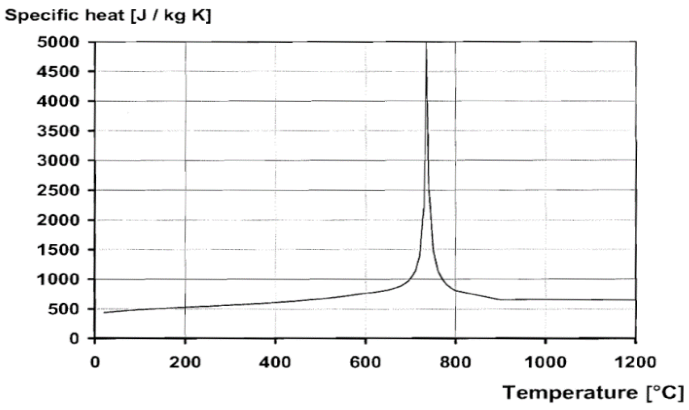

Figure 8. The specific heat of steel at high temperatures [5].

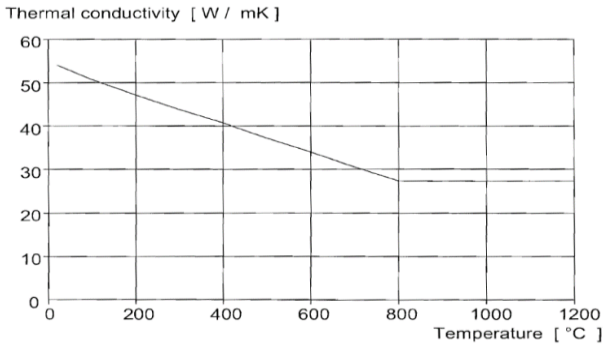

Figure 9. The specific heat of stainless steel at high temperatures [5]

Different fire curves (temperature-time relationships) significantly affect the response of the structure to fire. The fire curve of ISO 834 standard [36] is widely used in evaluating the structural behavior of isolated members in furnace experiments. In ABAQUS software [27], the geometry of steel frames is drawn. Fire analysis is considered as coupled temp displacement. In order to study the behavior of the studied frames, the nonlinear static analysis method is used as a lateral displacement application based on the reference paper [37]. The type of analysis is defined as "Static General." The distributed load is exerted to the surface of the beam in the frame as a compression of 60 kN, and then gradually, over a period of time, a fire load is applied to the structure. Since the strain stress curves entered in the software are a function of temperature, it is necessary to apply the initial temperature of 20 ° C to the structure from the initial step based on Figure 10.

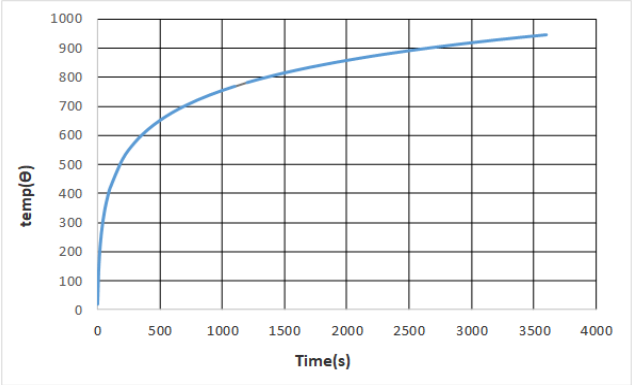

Figure 10. Curve of fire effect on the structure [2]

Also, the configuration of SMRF in ABAQUS software [27] is presented according to Figure 11. Based on Figure 12, in the mesh control section, the shape of all meshes is considered rectangular, and the "Structured" mesh method is considered; only in the partitioned part of the RBS sample flanges the meshing method is considered as "Free." Because the degree of freedom of the elements must be such that the simultaneous effects of temperature and displacement are taken into account, the "S4RT" element is used.

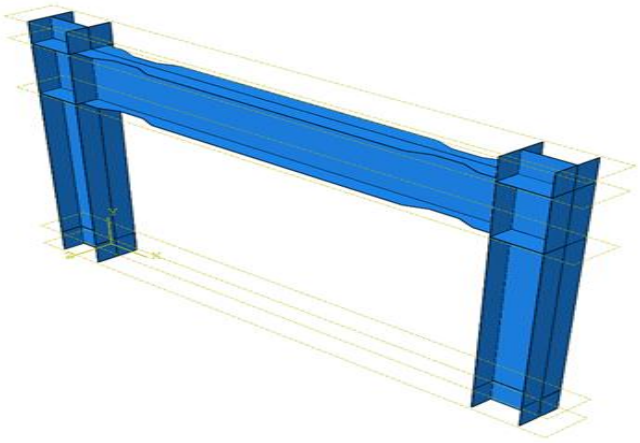

Figure 11. The configuration of *SMRF*.

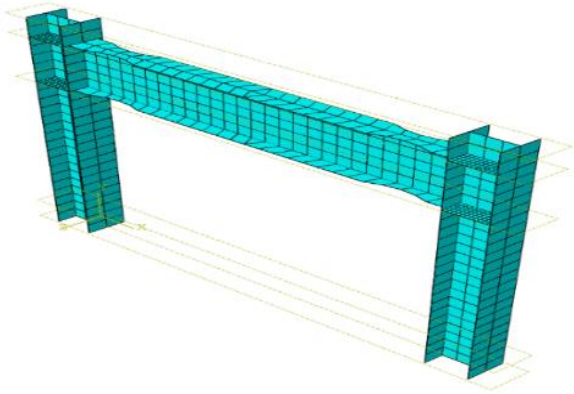

Figure 12. The Mesh of the general geometry of the model.

3. RESULTS AND DISCUSSION

3.1. THE OUTPUTS OF SAMPLES FRAME-RBS-01 AND FRAME-RBS-02

This section evaluates the effect of RBS connection with a radial section in samples Frame-RBS-01 and Frame-RBS-02. Then, the values of the final load in these samples at the end of fire analysis have been examined, and finally, in order to investigate the effects of stress and displacement of members resulting from the above-mentioned samples have been studied. Figure 13 indicates the maximum amount of stress in the allowable load range is equal to 459.7 MPa, and also, the values of displacement with increasing temperature in the connection are strongly increased so that the amount of vertical displacement in the middle of the span is equal to 113.2 mm for sample Frame-RBS-01 based on Figure 14. Meanwhile, the maximum stress and displacement are 449 MPa and 133.9 mm based on Figures 15 and 16, respectively, for sample Frame-RBS-02. According to Figures 17 and 18, the samples Frame-RBS-01 and Frame-RBS-02 can be tolerated and ruptured up to 747.57 ° C and 664.10 ° C, respectively. Therefore, increasing the load or fire exposure for a period of time, leads to an increase in the temperature of the structural elements and becomes completely ruptured.

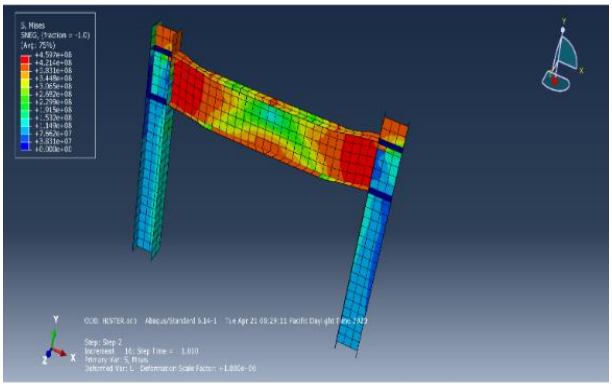

Figure 13. The counter of Von Mises stress sample Frame-RBS-01

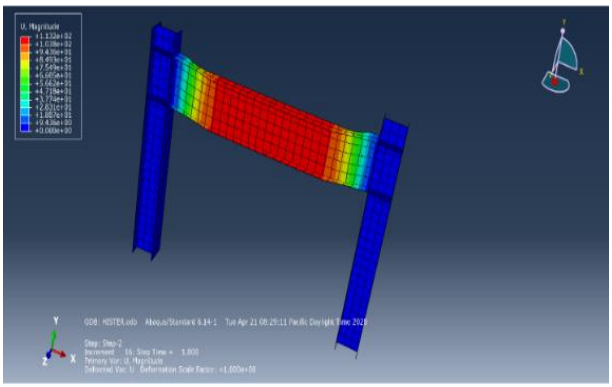

Figure 14. The Counter of displacement for sample Frame-RBS-01.

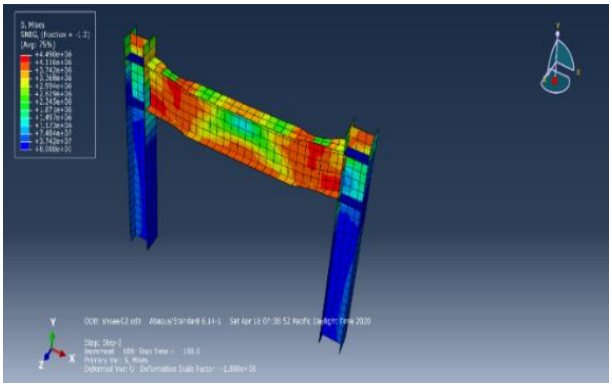

Figure 15. The counter of Von Mises stress sample Frame-RBS-02.

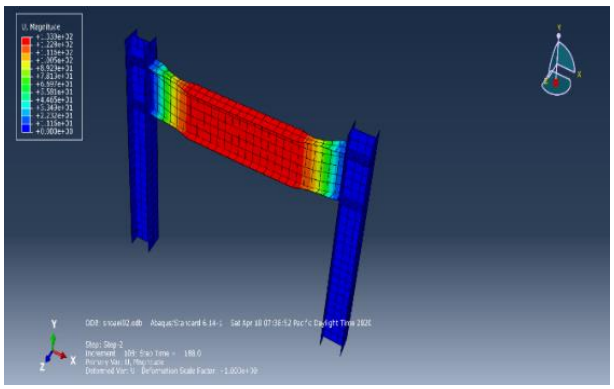

Figure 16. The Counter of displacement for sample Frame-RBS-02.

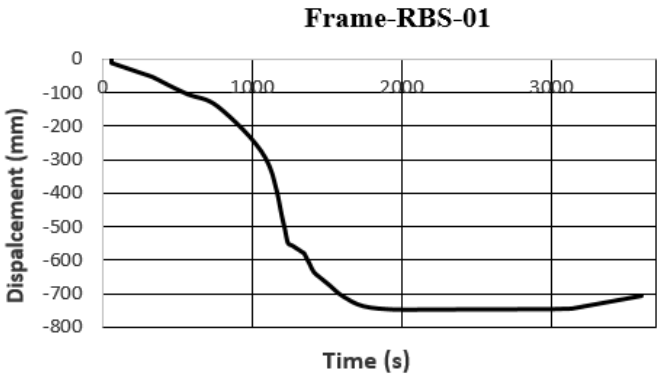

Figure 17. Displacement-time curve for sample Frame-RBS-01.

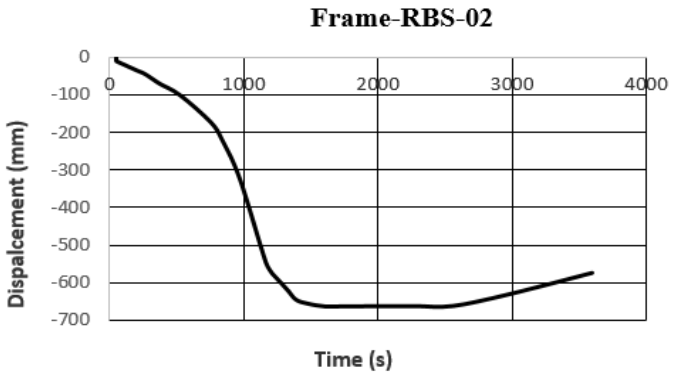

Figure 18. Displacement-time curve for sample Frame-RBS-02

3.2. OUTPUTS OF SAMPLES FRAME-RBS-RECTANGLE-01 AND FRAME-RBS-RECTANGLE-02

According to Figure 19, the maximum amount of stress in the allowable load range is 440 MPa, and the values of displacement with increasing temperature in the connection string are strongly increased so that based on Figure 20, the amount of vertical displacement in the middle of the span is 802.4 mm for Frame-RBS-Rectangle-01. Meanwhile, based on Figures 21 and 22, the maximum stress and displacement for sample Frame-RBS-Rectangle-02 are 440 MPa and 101.1 mm, respectively. Figures 23 and 24 show that the samples Frame-RBS-Rectangle-01 and Frame-RBS-Rectangle-02 may be endured and burst at temperatures of 623.79 ° C and 514.48 ° C, respectively.

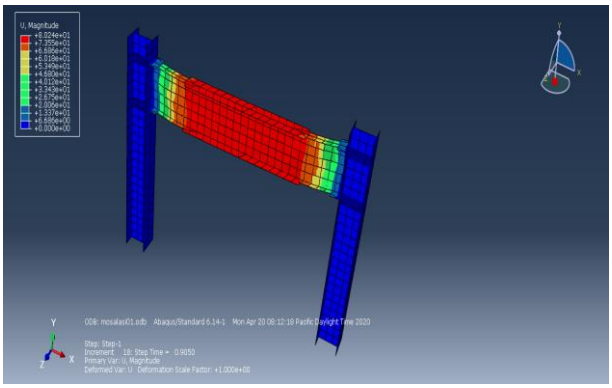

Figure 19. The counter of Von Mises stress sample Frame-RBS- Rectangle-01

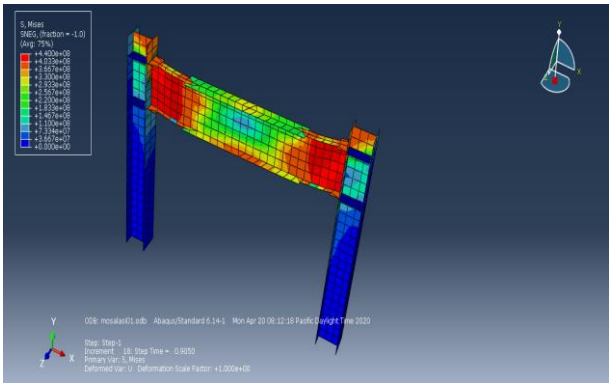

Figure 20. The Counter of displacement for sample Frame-RBS-Rectangle-01.

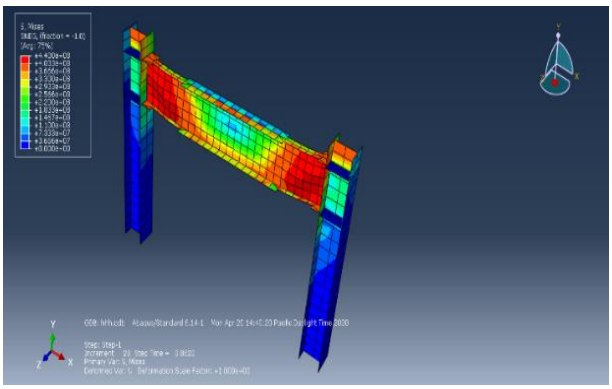

Figure 21. The counter of Von Mises stress sample Frame-RBS-Rectangle-02

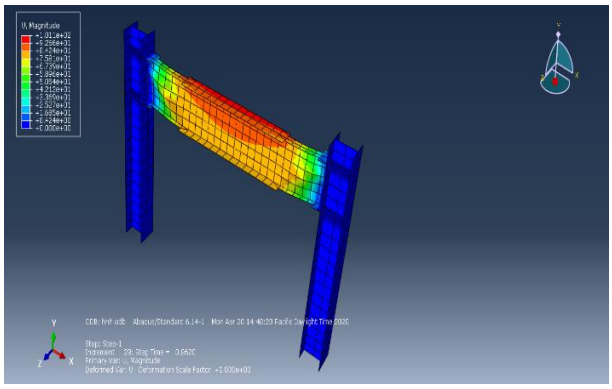

Figure 22. The Counter of displacement for sample Frame-RBS-Rectangle-02

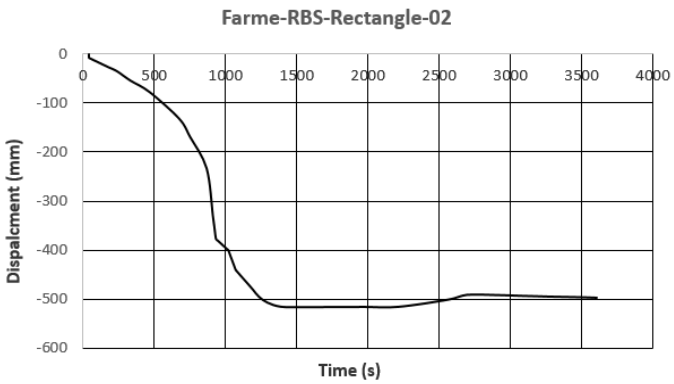

Figure 23. Displacement-time curve for sample Frame-RBS-Rectangle-01

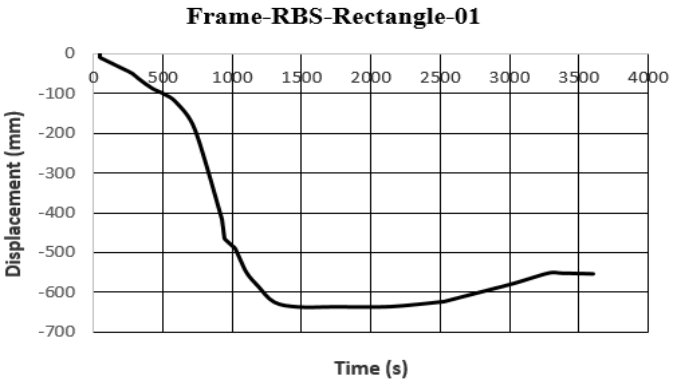

Figure 24. Displacement-time curve for sample Frame-RBS-Rectangle-02

3.3. THE OUTPUTS OF SAMPLES FRAME-RBS-TRIANGLE-01 AND FRAME-RBS-TRIANGLE-02

According to Figures 25 and 26, the maximum amount of stress in the allowable load range is 469.9 MPa, and the amount of displacement with increasing temperature in the connection is greatly increased so that the amount of vertical displacement in the middle of the span is equal to 166.6 mm. Based on Figure 27, from the beginning of loading until about 13 minutes later, under the influence of fire, deformation, and displacement occurred. Also, sample Frame-RBS-Triangle-01 can be tolerated and collapsed to 526/90 ° C, so by increasing the load or fire exposure for a period of time, which leads to an increase in the temperature of structural elements and suffers the rupture is complete. Based on Figures 28 and 29, the maximum amount of stress in the allowable load range is equal to 435.9 MPa, and the amount of displacement with increasing temperature in the connection string is greatly increased so that the amount of vertical displacement in the middle of the opening is equal to 222.1 mm for sample Frame-RBS-Triangle-02. Based on Figure 30, from the beginning of loading until about 14 minutes later, under the influence of fire, deformation, and displacement has been occurred. The sample Frame-RBS-Triangle-02 can withstand up to 598.63 ° C and break, so increasing the load or fire exposure for a period of time leads to an increase in the temperature of the structural elements.

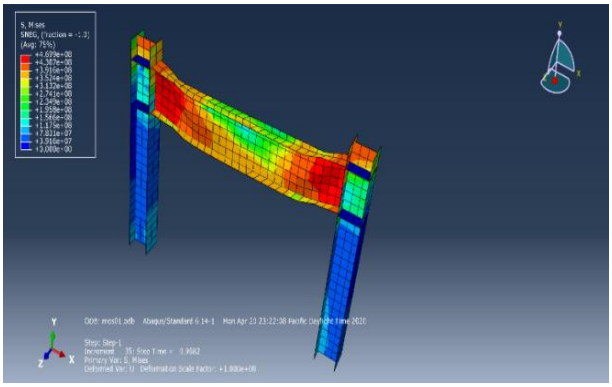

Figure 25. The counter of Von Mises stress sample Frame-RBS-Triangle-01.

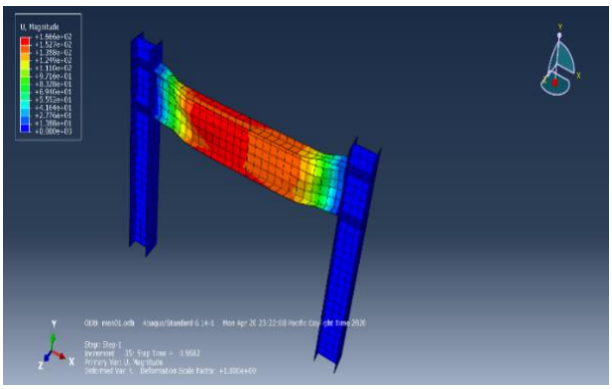

Figure 26. The Counter of displacement for sample Frame-RBS-Triangle-01.

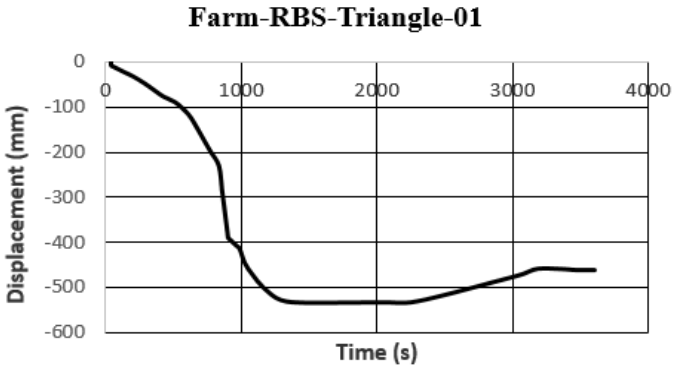

Figure 27. Displacement-time curve for sample Frame-RBS-Triangle-01.

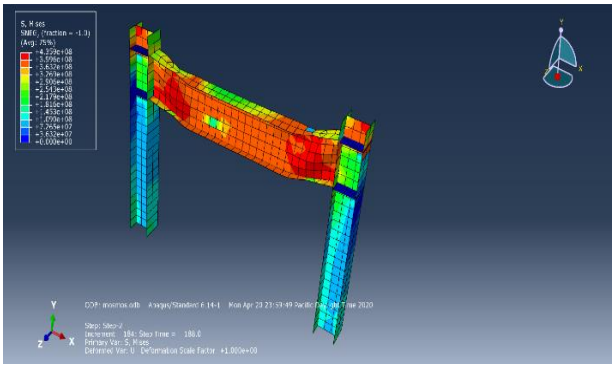

Figure 28. The Counter of Von Mises stress for sample Frame-RBS-Triangle-02.

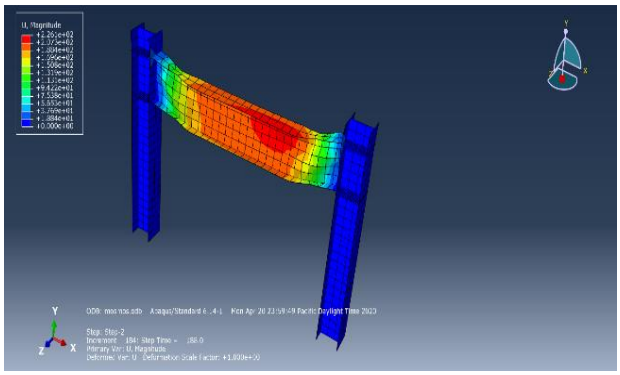

Figure 29. The Counter of displacement for sample Frame-RBS-Triangle-02.

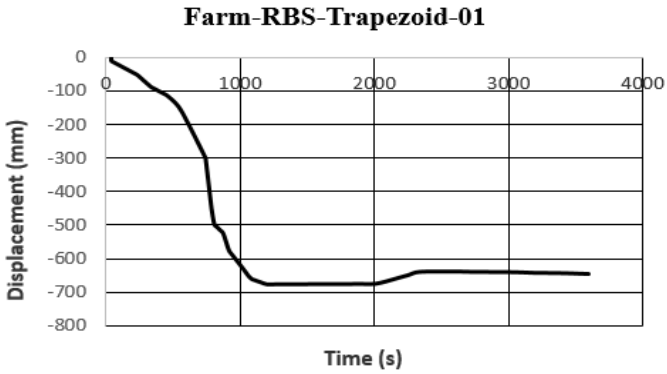

Figure 30. Displacement-time curve for sample Frame-RBS-Triangle-02.

3.4. OUTPUTS OF SAMPLES FRAME-RBS-TRAPEZOID-01 AND FRAME-RBS-TRAPEZOID-02

According to Figures 31 and 32, the maximum amount of stress in the allowable load range is equal to 462.5 MPa, and the amount of displacement with increasing temperature in the connection is greatly increased so that the amount of vertical displacement in the middle of the opening is equal to 334.8 mm. Based on Figure 33, it can be seen that from the start of loading until about 13 minutes later, under the influence of fire, deformation, and displacement has been occurred. In the following, the sample Frame-RBS-Trapezoid-01 can be tolerated and ruptured up to 673.99 ° C. Based on Figures 34 and 35, the maximum amount of stress in the allowable load range is equal to 448.9 MPa, and the values of displacement with increasing temperature in the connection are strongly increased so that the amount of vertical displacement in the middle of the opening is equal to 137 mm. According to Figure 36, it can be seen that from the beginning of loading until about 14 minutes later, deformation and displacement have occurred under the influence of fire conditions.

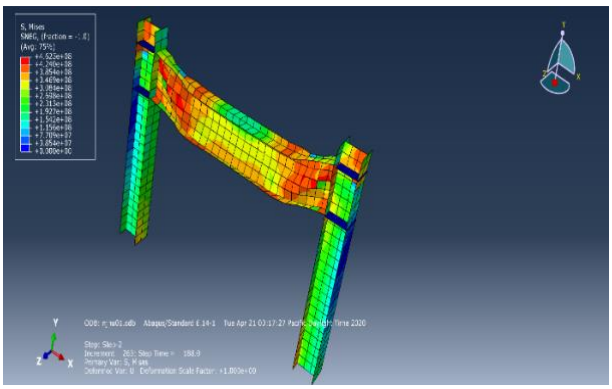

Figure 31. The counter of Von Mises stress sample Frame-RBS-Trapezoid-01.

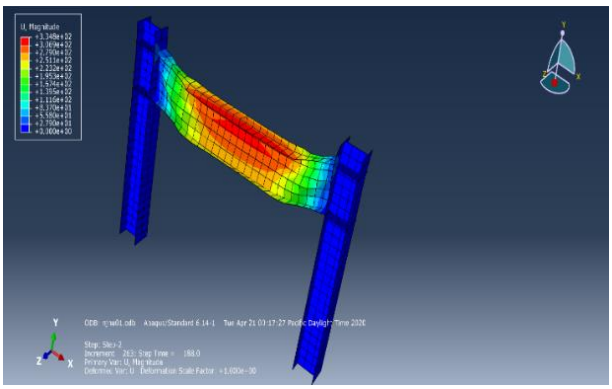

Figure 32. The Counter of displacement for sample Frame-RBS-Trapezoid-01.

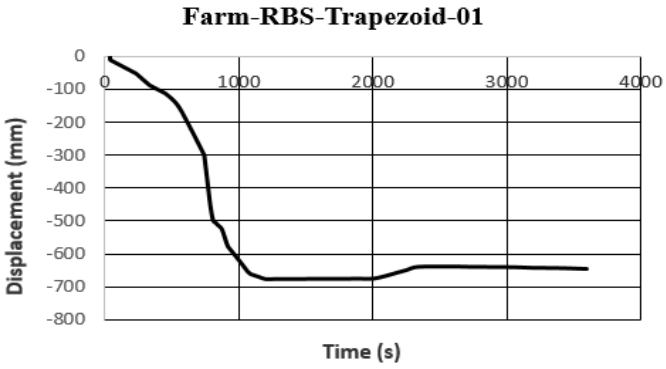

Figure 33. Displacement-time curve for sample Frame-RBS-Trapezoid-01.

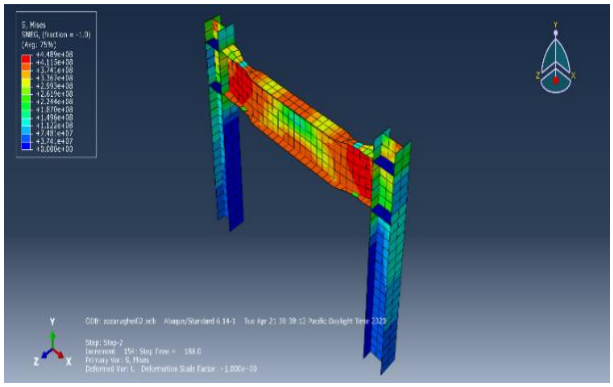

Figure 34. The counter of Von Mises stress sample Frame-RBS-Trapezoid-02.

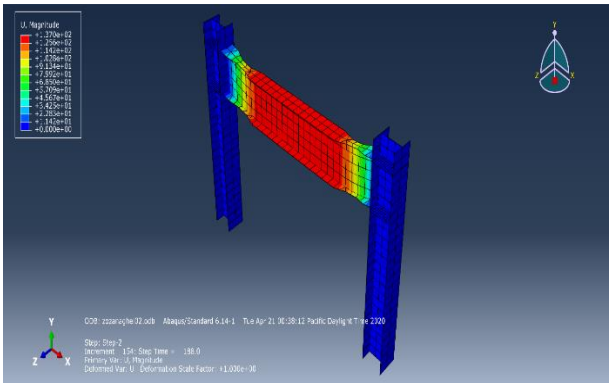

Figure 35. The Counter of displacement for sample Frame-RBS-Trapezoid-02.

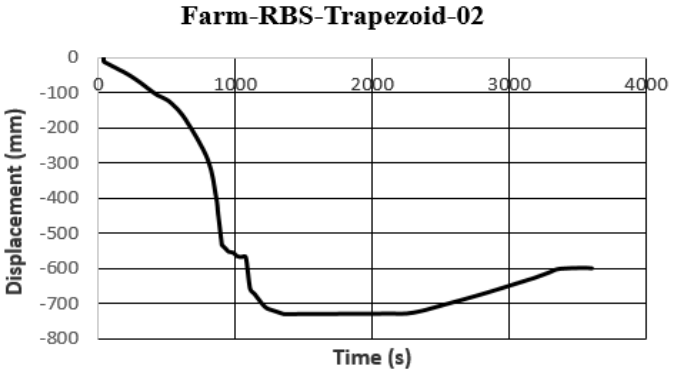

Figure 36. Displacement-time curve for sample Frame-RBS-Trapezoid-02.

3.5. DISCUSSION

One of the problems of fire engineering in construction is determining the moment of structural collapse. Given that a structure may be able to sustain some damage under fire conditions, it is hard to predict when the structure will collapse. Furthermore, in some constructions, the beams or columns bent during the fire, but the roofs and floors remained in place, and the structure did not collapse. As a result, a criterion to identify the breakdown of the building during a fire is required. According to Figure 37, for samples heated to 500 ° C, there is a significant reduction in ultimate strength. The ultimate length change for samples obtained from the web and flange of the profile increased as the temperature rose. The mechanical characteristics of the samples after fire reveal that their yield and ultimate strength fell considerably from 600 ° onwards, although their final strain rose. The elastic modulus for all samples does not change significantly with increasing temperature. As the temperature of the attenuated area increases, the longitudinal strain in these areas increases significantly and increases slowly outside the heated areas. In addition, the plastic joint transfer is better with increasing the temperature of the heated area. This indicates that the largest displacement applied is at both ends of the beam and at the column connection. Based

on Figure 37, sample Frame-RBS-01 has the highest ultimate strength compared to other samples up to 748.34 ° C. The lowest ultimate strength is for the sample Frame-RBS-Rectangle-02, which is up to 526.90 ° C. Meanwhile, sample Frame-RBS-Trapezoid-02 has the weakest performance versus other samples. Also, according to Figure 37, for samples heated to the range of 500 ° C, the ultimate strength of the change is significant, and a high drop in the ultimate strength is significant, too.

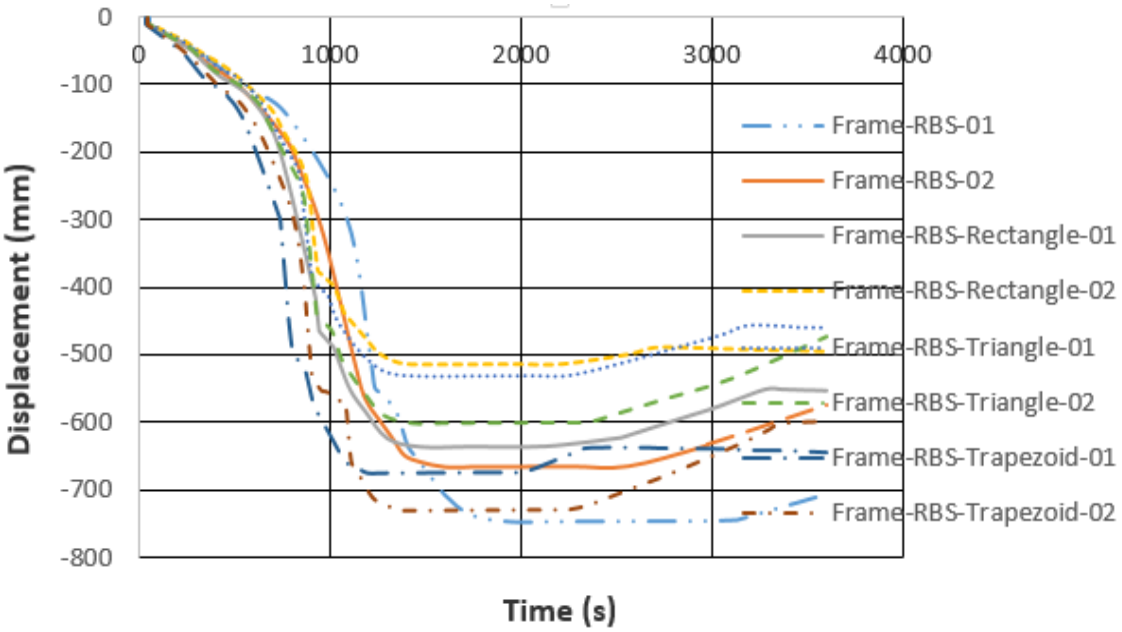

Figure 37. Displacement-time curve for all studied samples.

4. CONCLUSION

Fire and temperature rises in steel structures cause thermal stresses in steel and directly affect the behavior of steel. As the temperature increases, the strength and stiffness of the steel decrease, and its almost linear stress-strain curve becomes a nonlinear graph. This behavior of steel then affects the cross-sectional capacity as well as the behavior of the member. Increasing the temperature of the steel also affects the classification of the type of steel. In the present paper, the SMRF with RBS connections against fire has been investigated. Initially, previous research on SMRF with RBS connections was reviewed. ABAQUS finite element software was used for nonlinear analysis, and the accuracy of the proposed finite element modeling was compared to experimental results. In this paper, a total of four types of frames in the form of eight samples have been considered to evaluate the impact of RBS with cross-sectional radial, triangular, rectangular, and trapezoidal. The following outcomes can be extracted and presented: 1- European regulations are based on the design of structures at ambient temperature and provide coefficients of reduction of strength and stiffness for higher temperatures and do not explicitly consider the nonlinear strain stress behavior of steel at higher temperatures. Instead, a two-line model with a reduction in Young's modulus in elastic mode and a reduction in ultimate stress is considered for design purposes. 2- The stability and strength of the structure during fire conditions depend on many factors. One of the most important factors is the position and condition of the member in the structure, such as the ratio of member stress and how the member connects in the structure. 3- By increasing the temperature of the heated area, the transferring of the plastic hinge is conducted better. Meanwhile, based on the obtained outputs of displacement-time coefficients, the Frame-RBS-01 sample had the most ultimate strength compared to other samples up to 748.34 ° C temperature, and the least ultimate strength is related to the Frame-RBS-Rectangle-02 sample up to 526/90 ° C temperature. 4- If the temperature is high enough, the repair and reconstruction can reach the same rate with stiffness in tension. The result is that the hardening and softening of the steel balance each other and lead to a constant amount of stress. Theoretically, this stress range finally reaches all tensile hardening processes. The ductility of steel at ambient temperature is not high enough to reach this limit. As a result, failure occurs in steel. 5- In samples with rectangular cross sections, the amount of rupture is very high, so in the reduced parts, the stress is very high, and these samples do not bend.

FUNDING/SUPPORT

Not mentioned any Funding/Support by authors.

ACKNOWLEDGMENT

Not mentioned by authors.

AUTHORS CONTRIBUTION

This work was carried out in collaboration among all authors.

CONFLICT OF INTEREST

The author (s) declared no potential conflicts of interests with respect to the authorship and/or publication of this paper.

5. REFRENCES

[1] Adlparvar MR, Taghavi Parsa MH. The Improvement of the Tensile Behavior of CFRP and GFRP Laminates at Elevated Temperatures Using Fire Protection Mortar. Journal of Rehabilitation in Civil Engineering. 2021 May 1;9(2):41-54. [View at Google Scholar]; [View at Publisher].

[2] Chicchi R, Varma AH. Research review: Post-earthquake fire assessment of steel buildings in the United States. Advances in structural engineering. 2018 Jan;21(1):138-54. [View at Google Scholar]; [View at Publisher].

[3] Pouria Mirzaei P, Gerami M. Collapse assessment of protected steel moment frame under post-earthquake fire. Scientia Iranica. 2020 Dec 1;27(6):2775-89. [View at Google Scholar]; [View at Publisher].

[4] Ronagh HR, Behnam B. Investigating the effect of prior damage on the post-earthquake fire resistance of reinforced concrete portal frames. International Journal of Concrete Structures and Materials. 2012 Dec;6(4):209-20. [View at Google Scholar]; [View at Publisher].

[5] CEN, Eurocode 3: Design of Steel Structures, Part 1.2: General Rules – Structural fire design. (2005). European Committee for Standardization, Brussels. [View at Publisher].

[6] Eurocode 3, prEN-1993-1-8: 20, Part 1.8: Design of joints. Eurocode 3: Design of steel structures, draft2 rev. (2000). European Committee for Standardization, Brussels, Belgium. [View at Publisher].

[7] Muir L, Duncan CJ. The AISC 2010 specification and the 14th edition steel construction manual. InStructures Congress 2011 2011 (pp. 661-675). [View at Google Scholar]; [View at Publisher].

[8] Ali HM, Senseny PE, Alpert RL. Lateral displacement and collapse of single-story steel frames in uncontrolled fires. Engineering Structures. 2004 Apr 1;26(5):593-607. [View at Google Scholar]; [View at Publisher].

[9] Memari M, Mahmoud H, Ellingwood B. Post-earthquake fire performance of moment resisting frames with reduced beam section connections. Journal of Constructional Steel Research. 2014 Dec 1;103:215-29. [View at Google Scholar]; [View at Publisher].

[10] Behnam B, Ronagh HR. Post-Earthquake Fire performance-based behavior of unprotected moment resisting 2D steel frames. KSCE Journal of Civil Engineering. 2015 Jan;19:274-84. [View at Google Scholar]; [View at Publisher].

[11] Keller WJ, Pessiki S. Effect of earthquake-induced damage to spray-applied fire-resistive insulation on the response of steel moment-frame beam-column connections during fire exposure. Journal of fire protection engineering. 2012 Nov;22(4):271-99. [View at Google Scholar]; [View at Publisher].

[16] Sun Q, Guan C, Wang D. Study on mechanical characteristics and safety evaluation method of steel frame structure after fire. Theoretical and Applied Mechanics Letters. 2014 Jan 1;4(3):034006. [View at Google Scholar]; [View at Publisher].

[17] Strejček M, Řezníček J, Tan KH, Wald F. Behaviour of column web component of steel beam-to-column joints at elevated temperatures. Journal of Constructional Steel Research. 2011 Dec 1;67(12):1890-9. [View at Google Scholar]; [View at Publisher].

[18] Jiang B, Li GQ, Li L, Izzuddin BA. Simulations on progressive collapse resistance of steel moment frames under localized fire. Journal of Constructional Steel Research. 2017 Nov 1;138:380-8. [View at Google Scholar]; [View at Publisher].

[19] Guo Z, Huang SS. Behaviour of restrained steel beam with reduced beam section exposed to fire. Journal of Constructional Steel Research. 2016 Jul 1;122:434-44. [View at Google Scholar]; [View at Publisher].

[20] Jiang B, Li GQ, Usmani A. Progressive collapse mechanisms investigation of planar steel moment frames under localized fire. Journal of Constructional Steel Research. 2015 Dec 1;115:160-8. [View at Google Scholar]; [View at Publisher].

[21] Gernay T, Gamba A. Progressive collapse triggered by fire induced column loss: Detrimental effect of thermal forces. Engineering Structures. 2018 Oct 1;172:483-96. [View at Google Scholar]; [View at Publisher].

[22] Khizab B, Sadeghi A, Hashemi SV, Mehdizadeh K, Nasseri H. Investigation the performance of Dual Systems Moment-Resisting Frame with Steel Plate Shear Wall Subjected to Blast Loading. Journal of Structural and Construction Engineering. 2021 Oct 23;8(8):102-27. [View at Google Scholar]; [View at Publisher].

[23] Miryoysefi Aval SM, Shakeri K. Stability of steel moment resisting frames under fire loading. Journal of Structural and Construction Engineering. 2021 Aug 23;8(Special Issue 2):150-70. [View at Google Scholar]; [View at Publisher].

[24] Ghasemi, A. Evaluation of the performance of special steel moment frames under fire conditions. Journal of Structural and Construction Engineering, 2021, 4960125-134. (In Persian). [View at Google Scholar]; [View at Publisher].

[25] Sadeghi A, Kazemi H, Samadi M. Reliability and reliability-based sensitivity analyses of steel moment-resisting frame structure subjected to extreme actions. Frattura ed Integrità Strutturale. 2021 Jun 22;15(57):138-59. [View at Google Scholar]; [View at Publisher].

[26] Sadeghi A, Kazemi H, Samadi M. Single and multi-objective optimization of steel moment-resisting frame buildings under vehicle impact using evolutionary algorithms. Journal of Building Pathology and Rehabilitation. 2021 Dec;6:1-3. [View at Google Scholar]; [View at Publisher].

[27] ABAQUS Ins. ABAQUS Theory User Manual, V 6.7. (2007). [View at Publisher].

[28] Federal Emergency Management Agency (FEMA), FEMA 368. (2014). NEHRP recommended provisions for seismic regulations for new buildings and other structures. Washington (DC): Building Seismic Safety Council, Federal Emergency management Agency. [View at Publisher].

[29] FEMA 356. (2000). Pre-Standard and Commentary for the seismic Rehabilitation of Buildings. Washington D.C. Federal Emergency Management Agency, USA. [View at Publisher].

[30] Hwang JS., Ho SY. Modification on design formulas of structures with viscous dampers. Report no. NCREE-04-009. Taipei (Taiwan): National Center for Research on Earthquake Engineering of Taiwan. (2014).

[31] Kuntal VS, Chellapandian M, Prakash SS. Efficient near surface mounted CFRP shear strengthening of high strength prestressed concrete beams–An experimental study. Composite Structures. 2017 Nov 15;180:16-28. [View at Google Scholar]; [View at Publisher].

[32] Cornell CA, Jalayer F, Hamburger RO, Foutch DA. Probabilistic basis for 2000 SAC federal emergency management agency steel moment frame guidelines. Journal of structural engineering. 2002 Apr;128(4):526-33. [View at Google Scholar]; [View at Publisher].

[33] Rahnavard R, Thomas RJ. Numerical evaluation of the effects of fire on steel connections; Part 1: Simulation techniques. Case Studies in Thermal Engineering. 2018 Sep 1;12:445-53. [View at Google Scholar]; [View at Publisher].

[34] Swati AK, Gaurang V. Study of steel moment connection with and without reduced beam section. Case Studies in Structural Engineering. 2014 Jun 1;1:26-31. [View at Google Scholar]; [View at Publisher].

[35] Rasoulizadeh F, Tavakoli D. The effect of impact load on steel frames under fire conditions. Journal of Structural and Construction Engineering. 2022 Jan 21;8(11):259-77. [View at Google Scholar]; [View at Publisher].

[36] ISO-834 “Fire resistance tests-elements of building construction”, International Standard ISO 834. (1975). [View at Publisher].

[37] Saberi H, Saberi V, Javan S, Sadeghi A. Evaluation the effect of number, material and configuration of bolts on rigid bolted connections under fire. Journal of Structural and Construction Engineering. 2022 Mar 21;9(1):130-52. [View at Google Scholar]; [View at Publisher].